Noise figure and gain temperature dependent of praseodymium-doped fiber amplifier by using rate equations

Article *in* Optics Communications · February 2010

DOI: 10.1016/j.optcom.2009.10.005

2 authors:

Abdel Hakeim M. Husein
Al-Aqsa University

Fady I. El-Nahal
Islamic University of Gaza

Optics Communications 283 (2010) 409–413

Contents lists available at ScienceDirect

Optics Communications

journal homepage: www.elsevier.com/locate/optcom

Noise figure and gain temperature dependent of praseodymium-doped fiber amplifier by using rate equations

Abdel Hakeim M. Husein [a,*], Fady I. El-Nahal [b]

[a] Al-Aqsa University, Physics Department, P.O. Box 4051, Gaza, Gaza Strip, Occupied Palestinian Territory
[b] Islamic University of Gaza, Electrical Engineering Department, Gaza, Gaza Strip, Occupied Palestinian Territory

ARTICLE INFO

Article history:
Received 30 May 2009
Received in revised form 10 August 2009
Accepted 3 October 2009

Keywords:
PEDFA
Gain
Noise
ASE
Noise figure

ABSTRACT

A theoretical study of the temperature dependent noise effects of praseodymium-doped fiber amplifiers (PEDFAs) has been examined. The Pr^{3+}-doped ZBLAN fiber amplifier pumped at 1017 nm and Pr^{3+}-doped GeGa-sulfied fiber amplifier pumped at 1028 nm are chosen. The temperature-dependent rate and propagation equation related to four-level system consideration which is based on the population difference among amplification levels has been used. The population difference depends on pump and signal powers, Boltzman factor K_B, cross-sections, noise figure (NF) and Pr^{3+} concentration. The numerical results obtained over the temperature range from −20 °C to + 60 °C are used to present an analytical expression for the signal gain and noise figure effects in PDFAs length and noise figure with input pump power. The amplified spontaneous emission (ASE) has been taken into account.

1. Introduction

Praseodymium Pr^{3+}-doped fiber amplifiers (PDFAs) are now attracting more interest, because they expected to play a vital role in upgrading 1.3 μm optical systems that are used in almost all terrestrial optical telecommunication networks [1]. The erbium-doped fiber amplifiers (EDFAs) are widely used in the 1.55 μm window so a wider band WDM that would cover the band from 1.3 to 1.55 μm can be achieved [2]. The great interest in 1.3 μm amplifiers results from the fact that an important part of the fiber optic network worldwide use the 1.3 μm second communication window. PDFAs can provide substantial gain in this region. PDFA having the quantum efficiency of the $^1G_4 \rightarrow {}^3H_5$ transition in the 1.3 μm wavelength region has been demonstrated to be a good candidate for 1.3 μm communication window [2–5]. For this point, the low-phonon-energy glass hosts are needed to examine the amplifier span and all optical link-capacity.

Recently, some efforts have been methodically made to develop these types of optical amplifiers for utilizing over a wide range of temperatures. Especially, one major issue of PDFA research is to develop the gain efficiency with low noise figure (NF) of PDFA using **ZBLAN** (**Z**rF4, **B**aF2, **L**aF3, **A**lF3, **N**aF) fluoride, sulfide (**GeGaS**) and some borate-based glasses as a host material [6–9]. In addition, the temperature dependence of the gain characteristics of PDFAs is critical for these systems.

The increasing of the signal gain efficiency of the PDFAs amplifier has been the focus of current researches, controlling the temperature and selecting an appropriate host material. A practical fiber amplifier model can be used to realize the amplification procedure and examine the temperature dependence of PDFAs. The well-known temperature-dependent phenomena includes the temperature dependence of the stimulated emission cross-section spectra and the lifetime of the amplification level [10]. Another important description is the energy levels which are responsible for the amplification are split into many sub-levels and form energy bands. These sub-levels are caused by the splitting of an energy level under the local electric field around the rare earth ions doped to the host material. This splitting procedure is known as the Stark effect. A thermal distribution of population within the Stark sub-levels causes a partial change in the signal gain. On some theoretical works the temperature dependence of the signal gain in PDFAs has been explained, the temperature dependent analytic terms have not been given in expressions of the rate equation model including the Boltzmann factor to understand the influence of transitions $^3F_4 \leftrightarrow {}^3F_3$ on PDFA gain characteristics. In previous theoretical research, the dependence of the signal gain on the temperature of PDFAs has been examined from only the knowledge of stimulated emission cross section and lifetime of $^1G_4$.

In this work, the modified rate equation model will examine the effect of temperature on the signal gain. The main subject of this article is to find the noise figure of PDFA amplifier after solving the rate equation by including the temperature effect observed on the transitions $^3F_4 \leftrightarrow {}^3F_3$. The numerical results are given for

* Corresponding author. Tel.: +970 599165678; fax: +970 82865309.
E-mail address: hakeim00@yahoo.com (A.H.M. Husein).

0030-4018/$ - see front matter © 2009 Elsevier B.V. All rights reserved.
doi:10.1016/j.optcom.2009.10.005

both Pr^{3+}-doped fluoride based ZBLAN and Pr^{3+}-doped germanium-based sulfide fiber amplifiers, operating at the 1.3 μm signal wavelength and over the temperature range from −20 °C to +60 °C.

2. Theory

The set up of four-level absorption and radiation transitions of Pr^{3+} can be modeled based on the energy diagram shown in Fig. 1. This figure shows a simple four-level amplification system for PDFAs and main transitions between its spectroscopically visible energy levels which are labeled as $^1G_4$, $^3P_0$, $^1D_2$, $^3F_4$, $^3F_3$, $^3H_5$ and $^3H_4$ [11,12–15]. Also it includes the effect of the excited state absorption (ESA) to have better accuracy. The glass hosts with Pr^{3+} ions, five possible transitions can be taken into account to determine the population distribution of each level. The first two situations belong to $^1G_4 \leftrightarrow {}^3H_4$ transitions including the stimulated absorption and emission rates are R_{03} and R_{30}, respectively, for the pump powers transitions at wavelength close to 1017 nm or 1028 nm.

The other transitions belong to ground state absorption (GSA) including $^3H_4 \rightarrow {}^3F_4$ and the signal emission $^1G_4 \rightarrow {}^3H_5$ of signal photons. The transition rates of these processes are S_{02} and $S_{31,}$ respectively, belong to GSA and signal emission of signal, respectively.

In addition, the population of the $^1G_4$ level can be reduced by the cooperative upconversion caused by the $^1G_4 \rightarrow {}^1D_2$ and the $^1G_4 \rightarrow {}^3H_5$ transitions. This results from the fact that the energy difference between $^1G_4$ and $^1D_2$ levels matches the difference of $^1G_4$ and $^3H_5$ levels.

In the modeling of the four-level Pr^{3+} for 1.3 μm amplifications shown in Ref. [1], the non-radiative plus radiative spontaneous emission rates of the relevant levels are γ_{21}, γ_{10}, γ_{53}, γ_{43} and γ_{31} ($=1/\tau$).

The lifetime of the $^1G_4 \rightarrow {}^3H_5$ transition τ is an important quantity to evaluate the amplifier performance since, if it is short, it then becomes necessary to pump very hard to maintain a population inversion.

The population of levels is labeled as N_0, N_1, N_2, N_3, N_4 and N_5, respectively, and also the total population density N is taken as $N = N_0 + N_1 + N_2 + N_3 + N_4 + N_5$. In this point, the special names of

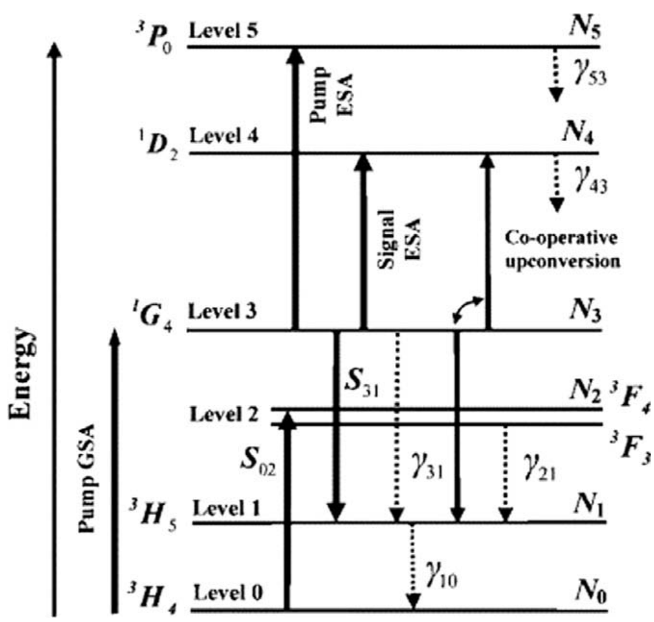

Fig. 1. Pr^{3+} energy levels and main transition in several glass hosts (not to scale).

N_3 and N_0 are the population densities of metastable and ground levels, respectively.

To calculate all of the population of Pr^{3+} at steady state conditions, the effects of pump ESA and the cooperative upconversion are not taken into consideration.

However, this consideration confirms that the upconversion mechanism in Pr^{3+}-doped glass is negligible at concentration level below ∼1000 ppm and at temperatures below ∼350 K. So, the effects we consider in the used temperature-sensitive model are just GSA (R_{03}) and the stimulated emission (R_{30}) of pump photons, and the stimulated absorption (S_{02}), stimulated emission (S_{31}) and ESA (S_{34}) of signal photons.

The simplified energy level diagram (four-level $^1G_4 \rightarrow {}^3H_5$ transition of Pr^{3+} for 1.3 μm) is shown in Fig. 2, taking into account the Boltzmann distribution of transitions $^3F_4 \leftrightarrow {}^3F_3$.

N_{22} and N_{21} denote the population densities of Pr^{3+} ions within the sub-levels of the second energy level. In the fact, this system contains many sub-levels where the praseodymium-ions reside. These sub-levels are unequally populated due to the thermal distribution of ions. Therefore, the thermal equilibrium and the relative population of the sub-levels are arranged as a function of temperature and governed by Boltzman's distribution law. This type has been studied by Berkdemir et al. [16]

$$\beta = \frac{N_{22}}{N_{21}} = \frac{C_{nr}^{+}}{C_{nr}^{-}} = \exp\left(-\frac{\Delta E}{K_B T}\right) \tag{1}$$

where β is the Boltzmann population factor, K_B is Boltzmann's constant which equals 0.596 cm^{-1}/K, T is the temperature in Kelvin degree, C_{nr}^{+} and C_{nr}^{-} are the non-radiative rates that correspond to thermalization process which is occurring within manifold of the second level and $\Delta E = E_{22} - E_{21}$ is the energy difference between $^3F_4 \rightarrow {}^3F_3$ transitions, and is on the order of a few hundred cm^{-1} [17]. On the basis of the energy level diagram shown in Fig. 2, and using upper conditions, the rate equation for Pr^{3+} population density can be written as follow

$$\frac{dN_3}{dt} = R_{03}N_0 - R_{30}N_3 - \gamma_{332}N_3 \tag{2}$$

$$\frac{dN_2}{dt} = \frac{dN_{22}}{dt} + \frac{dN_{21}}{dt} = S_{021}N_0 - S_{221}N_{22} - \gamma_{221}N_{22} + \gamma_{322}N_3 \tag{3}$$

$$\frac{dN_1}{dt} = S_{221}N_{22} + \gamma_{221}N_{22} - \gamma_{10}N_1 \tag{4}$$

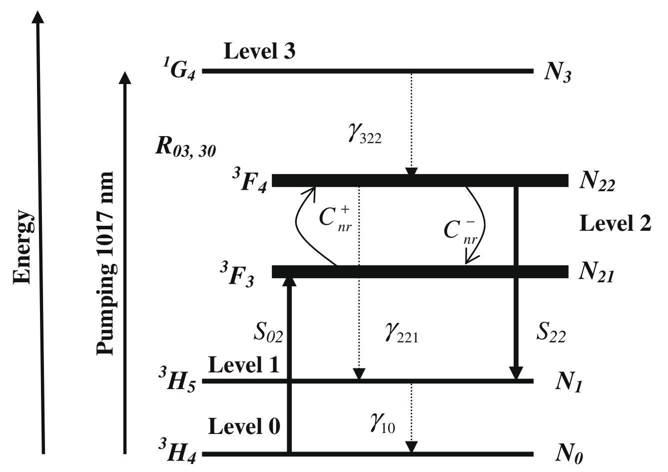

Fig. 2. Simplified energy level diagram concerning four-level amplification system and main transition of praseodymium ion in glass hosts.

$$\frac{dN_0}{dt} = R_{30}N_3 - R_{03}N_0 - S_{021}N_0 + \gamma_{10}N_1 \tag{5}$$

The rate equation are solved under the condition of steady state regime, where all of the levels are time invariant, i.e., $dN_i/dt = 0$, ($i = 0, 1, 21, 22, 3,\ldots$)

$$\frac{dN_0}{dt} = \frac{dN_1}{dt} = \frac{dN_{22}}{dt} + \frac{dN_{21}}{dt} = \frac{dN_3}{dt} = 0 \tag{6}$$

To simplify the model, we assumed that the population of level 1 is close to zero because practically the non-radiative transition from level 1 to 0 is much faster than any other transitions. In other words, N_1 is taken as zero due to the level 1 relaxes instantaneously to the level 0. Also by assuming transitions from level 3 to 2 and from level 1 to 0 are predominantly non-radiative and thus the radiative transitions from these level can be neglected, so $R_{30}N_3 = 0$ and $S_{021}N_0 = 0$. Therefore, the total population density N can be considered as

$$N \approx N_0 + N_{22} + N_{21} \tag{7}$$

From Eq. (1), Eq. (7) can be wrote in terms of β as

$$N \approx N_0 + (1 + 1/\beta)N_{22} \tag{8}$$

The population N_{22} of the $^3F_4$ level of the Pr^{3+} is obtained by solving Eqs. (2) and (3) and using Eqs. (6) and (8). The temperature dependent results is

$$N_{22} = Nx\frac{\frac{\sigma_{03}\Gamma_p}{h\upsilon_p A}P_p\tau}{1 + \tau\left[\frac{\sigma_{03}\Gamma_p}{h\upsilon_p A_p}P_p(1 + 1/\beta) + \frac{\sigma_{221}\Gamma_s}{h\upsilon_s A_s}P_s\right]} \tag{9}$$

where $R_{03} = \frac{\sigma_{03}\Gamma_p}{h\upsilon_p A_p}P_p$, $S_{221} = \frac{\sigma_{221}\Gamma_s}{h\upsilon_s A_s}P_s$, σ_{03} is the stimulated absorption of Pr^{3+} transitions $^3H_4 \leftrightarrow {}^1G_4$, σ_{221} is the stimulated emission cross section of transitions $^3H_4 \rightarrow {}^3H_5$ at wavelength, υ_p and υ_S are the pump and signal frequencies, respectively, P_p and P_s are the pump and signal powers, respectively, Γ_p and Γ_s are the overlap factors; A_p and A_s are the effective doped areas of the core corresponding to pump and signal powers, respectively, and h is Planck's constant.

The signal gain of PDFA depends only on transitions between two levels which have the population densities N_{22} and N_0. When a signal light beam with power P_s at wavelength λ_s traverses through an amplification medium of extremely small thickness dz, the change of power dP_s is given by the following propagation equation:

$$\frac{dp_s}{dz} = (\sigma_{221}N_{22} - \sigma_{021}N_0)\Gamma_s P_s \tag{10}$$

where σ_{221} is the stimulated absorption cross section of the Pr^{3+} $^3H_4 \rightarrow {}^3F_4$ transition at the signal wavelength. The solution of Eq. (10) for a length L is written as

$$G = \frac{P_s(L)}{P_s(0)} = \exp\left[\Gamma_s\sigma_{221}N_{22}L\right] \tag{11}$$

where L represents the length of Pr^{3+}-doped amplifier and G denotes the signal gain. The Gain in decibel (dB) can be written as

$$G(dB) = 10\log_{10}\exp\left[\Gamma_s\sigma_{221}N_{22}L\right] \tag{12}$$

By neglecting the term including fiber ground state absorption $\sigma_{021}N_0$ as it represents loss due to unexcited ions which is bleached in highly excited amplifier.

In the general situation, a model of PDFA will be helpful for the system design which requires knowledge about the signal gain and amplified spontaneous emission (ASE) in terms of operating wavelength, and input power. When the signal gain increases, the ASE noise power increases accordingly.

The noise figure, NF, of the amplifier is defined as then degradation in signal-to-noise ratio from input to output of the amplifier, NF is given by:

$$NF = \frac{1}{G}\left(1 + \frac{P_{ASE}\Delta\upsilon}{GP_{in}}\right) + \frac{1}{G}\frac{P_{ASE}}{h\upsilon_s}\left(1 + \frac{P_{ASE}\Delta\upsilon}{2GP_{in}}\right) \tag{13}$$

where $(1/G)$ is the signal-spontaneous beat noise, P_{ASE} is the ASE power density, P_{in} is the signal power density, υ_s is the frequency of the input signal, and $\Delta\upsilon$ is the optical linewidth of the amplifier. The NF can be given in decibel (dB) as follows;

$$NF(dB) = 10\log_{10}\left[\frac{1}{G}\left(1 + \frac{P_{ASE}\Delta\upsilon}{GP_{in}}\right) + \frac{1}{G}\frac{P_{ASE}}{h\upsilon_s}\left(1 + \frac{P_{ASE}\Delta\upsilon}{2GP_{in}}\right)\right] \tag{14}$$

3. Results and discussion

For numerical calculation, the fiber parameters for Pr^{3+}-doped sulfide and ZBLAN amplifiers are taken from Refs. [13,14]. The parameters and their values used in calculation are shown in Table 1. As can be noted from Table 1, the stimulated emission cross section of GeGa-sulfide glass is larger than the cross section of ZBLAN one. This is due to the GeGa-sulfide glass has a calculated quantum efficiency of 59% where the value reported for ZBLAN glass is 3.4% at 1310 nm [10,18]. Here we present the simulation results for both Pr^{3+}-doped sulfide and ZBLAN amplifiers, where we used the input signal power 1 mW (−30 dB).

At room temperature for simplicity, the energy interval between N_{22} and N_{21} levels of GeGa-sulfide and ZBLAN-based Pr^{3+} ions are assumed to be close to 500 and 400 cm^{-1}, respectively. The values of β calculated over the temperature range from −20 °C to 60 °C by Eq. (1) are given in Table 2.

3.1. Gain and noise figure versus length

Firstly we studied the variation of gain and noise figure (NF) with the length of the amplifier for both GeGa-sulfide-based and ZBLAN-based Pr^{3+}-doped fiber amplifiers over the temperature range from −20 °C to 60 °C. The results for the GeGa-sulfide based amplifier are shown in Figs. 3 and 4, respectively, while the ZBLAN amplifier results are shown in Figs. 5 and 6, respectively. It is clear from the results that the signal gain rises with increases in the length, at the same time the gain declines when the temperature increases. However the NF decreases with increasing the length. Furthermore, the NF increases when the temperature rises. It can be noticed that longer ZBLAN amplifier is needed to produce the same gain of that of GeGa-sulfide-based amplifier. For example to achieve a signal gain of 20 dB at 20 °C, a 5 m long GeGa-sulfide based amplifier is sufficient while a 32 m long ZBLAN amplifier is needed to achieve the same gain.

Table 1
Parameters and their values used in calculations for the Pr^{3+}-doped sulfide and ZBLAN fiber amplifiers.

Parameters	GeGa-sulfide Ref. [12]	ZBLAN Ref. [13]
σ_{03}	9.7×10^{-26} m^2	4.24×10^{-26} m^2
σ_{221}	–	1.2×10^{-26} m^2
τ	360 µs	110 µs
N	7.82×10^{25} m^{-3}	4.80×10^{25} m^{-3}
λ_s	1310 nm	1300 nm
λ_p	1028 nm	1017 nm
A_s, A_p	15.40 µm^2, 12.30 µm^2	8.04 µm^2
Γ_s, Γ_p	0.38, 0.40	0.60
L	8 m	36 m

Table 2
β Values as a function of temperature for the relevant fiber amplifiers.

Temperature (°C)	β (for GeGa-sulfide)	β (for ZBLAN)
−20	0.058	0.103
0	0.072	0.121
+20	0.086	0.140
+40	0100	0.159
+60	0.115	0.177

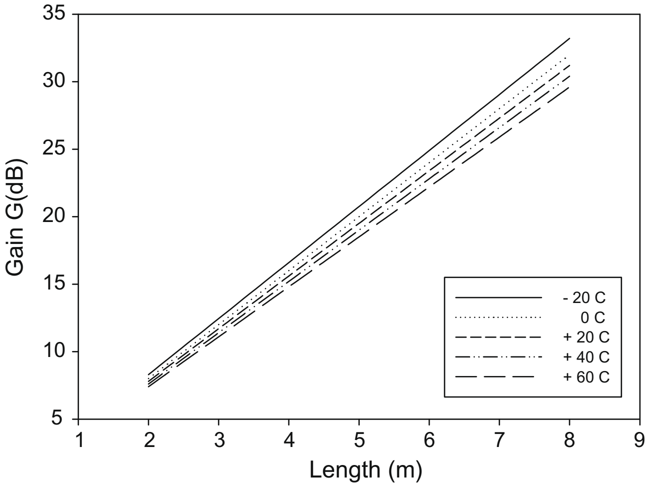

Fig. 3. The change of the signal gain with temperature and length of GeGa-sulfide based Pr^{3+}-doped fiber amplifier for a signal input power of −30 dBm and pump power of 20 dBm.

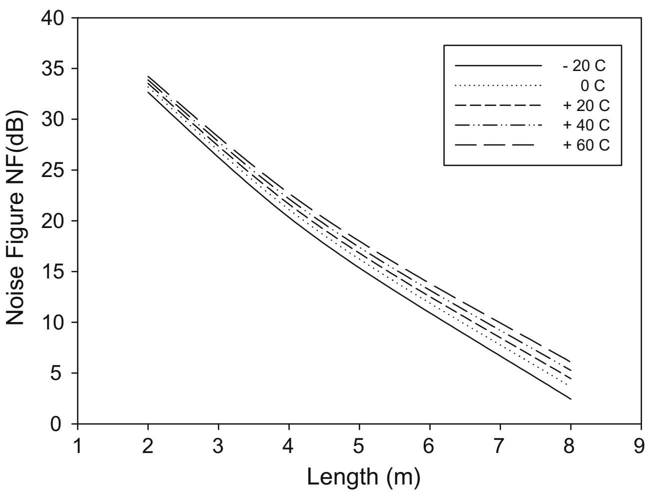

Fig. 4. The change of the noise figure with temperature and length of GeGa-sulfide based P^{3+}-doped fiber amplifier for a signal input power of −30 dBm and pump power of 20 dBm.

3.2. Noise figure versus pump power

Previous work has studied the variation of signal gain with pump power over several temperatures [16]. The gain results obtained here confirm these results. Here we studied the dependence of NF on the pump power over the temperature range from −20 °C to 60 °C. The results are shown in Fig. 7 for GeGa-sulfide based amplifier at length of 8 m and input signal power −30 dB and Fig. 8 for ZBLAN amplifier at length of 36 m and input signal power −30 dB, respectively. It is clear that the NF decreases with increase the pump power. At the same time it can be noticed that the NF

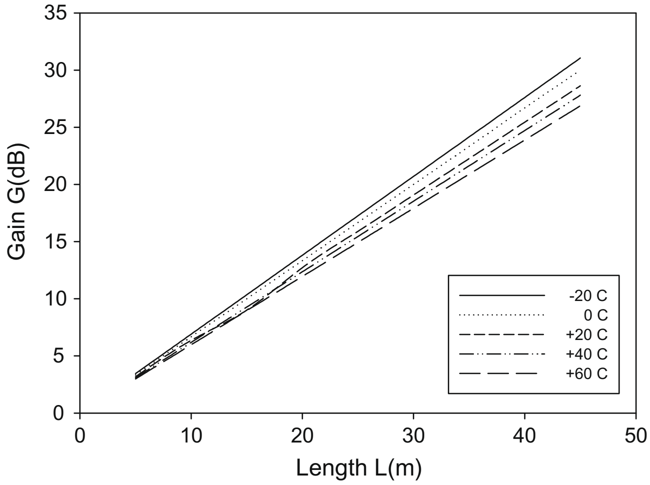

Fig. 5. The change of the signal gain with temperature and length of ZBLAN-based Pr^{3+}-doped fiber amplifier for a signal input power of −30 dBm and pump power of 20 dBm.

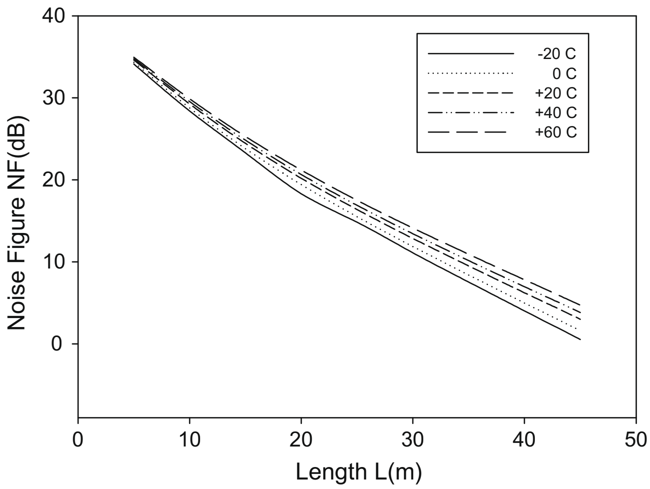

Fig. 6. The change of the noise figure with temperature and length of ZBLAN-based P^{3+}-doped fiber amplifier for a signal input power of −30 dBm and pump power of 20 dBm.

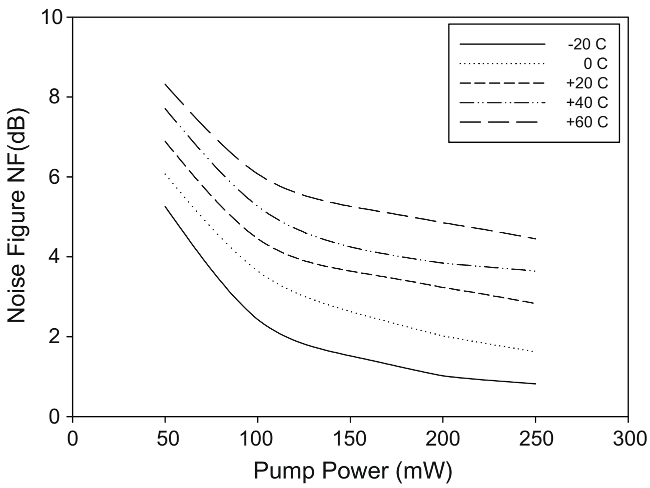

Fig. 7. The change of noise figure with temperature and pump power in GeGa-sulfide-Pr^{3+}-doped fiber amplifier for a signal input power of −30 dBm.

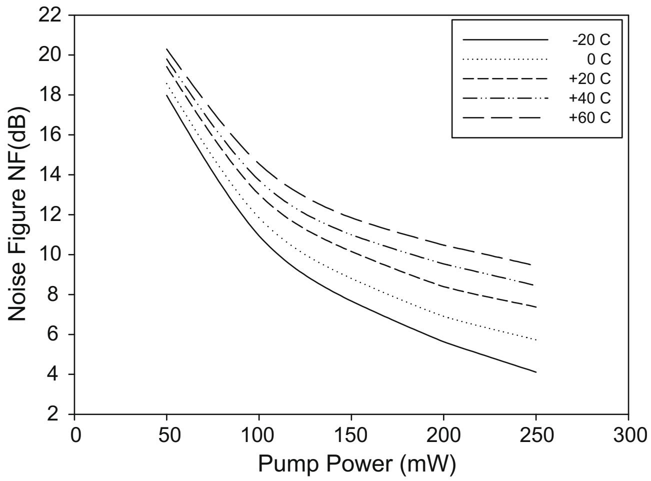

Fig. 8. The change of noise figure with temperature and pump power in ZBLAN-based Pr^{3+}-doped fiber amplifier for a signal input power of −30 dBm.

increases with increases temperatures range. It can be seen from the results that GeGa-sulfide based amplifier is more stable than ZBLAN amplifier. For example, when the pump power is 250 mW, the NF rises from 0.82 dB to 4.45 dB when the temperature rises from −20 °C to 60 °C for GeGa-sulfide-based amplifier. For the same pump power, the NF rises from 4.1 to 9.43 dB with the same temperature change for ZBLAN amplifier.

4. Conclusion

A PDFA model has been introduced including the temperature effects for gain and noise figure of a length of the praseodymium-doped fiber amplifier for two types ZBLAN and GeGa-sulfied. Also the model has included the change of noise figure with the variation of input pump power of PDFA. The amplified spontaneous emission (ASE) has been taken into account as a part of the noise figure. The temperature dependence of the gain and noise figure on various temperatures was taken into consideration which shows that the performance of PDFA depends on the temperature. The analytical solution of the propagation equations has also been derived for the temperature range from −20 °C, to +60 °C for finding the gain.

References

[1] Y. Ohishi et al., Opt. Lett. 16 (22) (1991) 1747.
[2] G. Lawton, Optical Amplifiers Technology and System, IGI Publisher, 1999.
[3] Y. Ohishi et al., OFC91, Postdeadline Paper PD2, 1991
[4] Y. Miyajima et al., Top. Meet. Opt. Amp. Appl., Postdeadline Paper PD1, 1991
[5] B. Pedersen, W.J. Miniscalco, R.S. Quimby, IEEE Photon. Technol. Lett. V. 4 (5) (1992) 446.
[6] S.H. Yuan, J. Non-Cryst. Solids 215 (1997) 108.
[7] K. Itoh et al., J. Non-Cryst. Solids 256–257 (1999) 1.
[8] D.R. Simons, A.J. Faber, H. de Waal, Opt. Lett. 20 (5) (1995) 468.
[9] P. Sirivastava, S.B. Rai, D.K. Rai, J. Alloys Compd. 368 (2004) 1.
[10] Y. Ohishi et al., Opt. Lett. 20 (4) (1995) 383.
[11] K. Isshiki et al., IEEE J. Lightwave Technol. 16 (12) (1998) 2373.
[12] L.B. Shaw, B.B. Harbison, B. Cole, J.S. Sanghera, I.D. Aggarwal, Opt. Express 1 (4) (1997) 87.
[13] D.R. Simons, Eindhoven University of Technology Research Reports, ISBN: 90-386-0496-3, November 1995.
[14] Y. Ohishi, T. Kanamori, Y. Terunuma, M. Shimizu, M. Yamada, S. Sudo, IEEE Photon. Technol. Lett. 6 (2) (1994) 195.
[15] J. Wu, S.L. Tsao, C.H. Ho, J. Opt. Commun. 24 (6) (2003) 223.
[16] Cuneyt Berkdemir, Sedat Ozsoy, Opt. Commun. 269 (2007) 102–106.
[17] E. Desurvire, Erbium-doped Fiber Amplifiers: Principles and Applications, Wiley Interscience, New York, 1994.
[18] A.W.H. van Osch, Eindhoven University of Technology Research Reports, EUT Report 95-E-294, ISBN: 90-6144-294-X, October 1995.